Superconductivity and the valence state of the Sr site in defective $Bi_{1.8}Pb_{0.2}Sr_2CuO_y$

Yan Hongjie and Mao Zhiqiang
Structure Research Laboratory, University of Science and Technology of China, Hefei, 230026 Anhui, People's Republic of China

Zhang Yuheng
Chinese Center of Advanced Science and Technology (World Laboratory), P.O. Box 8730, Beijing, People's Republic of China and Structure Research Laboratory, University of Science and Technology of China, Hefei, 230026 Anhui, People's Republic of China

(Received 1 February 1999)

The superconductivity and the average valence state of the Sr site are comparatively investigated for the La-doped $Bi_{1.8}Pb_{0.2}Sr_{2-x}La_xCuO_y$ ($0.1 \leqslant x \leqslant 0.8$) system and Sr-vacant $Bi_{1.8}Pb_{0.2}Sr_{2-x}CuO_y$ ($0 \leqslant x \leqslant 0.6$) system. Electronic diffraction patterns and Raman spectra show that the incommensuration modulation (IM) is intensified in both systems, but the variation of the IM wavelengths in the La-doped system is much larger than in the Sr-vacant system. Resistivity measurements display that the superconductivity in the La-doped system appears from an overdoped region to underdoped region; however, it is strongly suppressed in the Sr-vacant system. Experimental analysis indicates that such differences between the two systems may arise from the fact that the La doping is pure electron filling, but the Sr vacancy in the Sr site brings about a shift of the apical oxygen of the CuO_6 octahedron and therefore the conductivity of the CuO_2 planes is directly influenced.

I. INTRODUCTION

The understanding of the mechanism of high-temperature superconductivity (HTSC) represents a formidable challenge for both theory and experiment. Large efforts have been taken, and many experiments have revealed that high-T_c superconductivity is closely related to the microstructure characteristics.[1–8] One of the common properties in different high-T_c cuprate systems is that the crystal structure is formed layer by layer. Different layers in the crystal structures possess different contribution to the high-T_c superconductivity:[9] the CuO_2 planes are conductive layers which are believed to mainly dominate the superconductivity and the normal-state transport properties, the double Bi_2O_2 layers in Bi-based systems from the Bi-concentrated band which is commonly considered to be the origin of the incommensurate modulation.[7,10] In the Bi2201 phase the SrO_2 layers are located between the upper Bi_2O_2 layers and the lower CuO_2 planes and directly coupled with the upper and lower layers. Simultaneously, the oxygen atom in the SrO_2 layer is just the apical oxygen of the CuO_6 octahedron. What role does the SrO_2 layer play in high-T_c superconductivity and how do changes in the SrO_2 layer influence the transport properties and the microstructure of the high-T_c cuprates? In the present work, we substituted the La for Sr in the Bi2201 phase, which should increase the average valence state in the Sr site, and introduced the Sr vacancy in the SrO_2 layers, which should decrease the average valence state in the Sr site. We expect to investigate how the changes of the average valence state in the Sr site influence the superconductivity and the microstructure in the Bi2201 phase. Our experimental results indicate that both La doping and Sr vacancy in the Sr site bring about a reduction of the incommensurate-modulation wavelengths in the two systems. La doping is pure electronic filling, and the superconductivity and the normal-state transport properties are mainly dominated by changes of the carrier concentration for the $Bi_{1.8}Pb_{0.2}Sr_{2-x}La_xCuO_y$ system. Nevertheless, Sr vacancy in the Sr site results in a shift of the apical oxygen of the CuO_6 octahedron in the $Bi_{1.8}Pb_{0.2}Sr_{2-x}CuO_y$ system and the conductivity of the CuO_2 planes is directly influenced. Therefore, superconductivity is strongly suppressed in the Sr-vacancy Bi2201 system.

II. EXPERIMENTAL METHODS

The preparation of polycrystalline samples of $Bi_{1.8}Pb_{0.2}Sr_{2-x}CuO_y$ ($0.0 \leqslant x \leqslant 0.6$) has been reported elsewhere.[11] The polycrystalline samples of $Bi_{1.8}Pb_{0.2}Sr_{2-x}La_xCuO_y$ ($0.0 \leqslant x \leqslant 1.0$) were synthesized by the conventional solid-state reaction technique using high-purity powders of Bi_2O_3, PbO, $SrCO_3$, La_2O_3, and CuO. The mixtures of these powders were well ground and calcined at about 900 °C for 12 h in air. In order to ensure that the mixtures react completely, the calcined powders were thoroughly reground and reheated 2 times in the above condition. The powders were pressed into pellets and sintered in air at 925 °C for 24 h. Finally, the samples were annealed at 600 °C for 17 h and furnace cooled to room temperature.

The resistivity was measured using a standard four-probe method in a closed-cycle helium cryostat within the measurement temperature range of 4.2–300 K. The resistivity measurements were automatically controlled by a computer. X-ray-diffraction (XRD) analyses were carried out with Rigaku-D/max-γA diffractometer using monochromatic high-intensity Cu $K\alpha$ radiation. Raman scattering spectra were measured on a Spex-1403 Raman spectrophotometer using a backscattering technique. The 5145-Å line from an argon-ion laser was used as an excitation light source. All measurements were performed at room temperature. Electron-diffraction (ED) patterns were obtained using an H-800 transmission electron microscope (TEM).

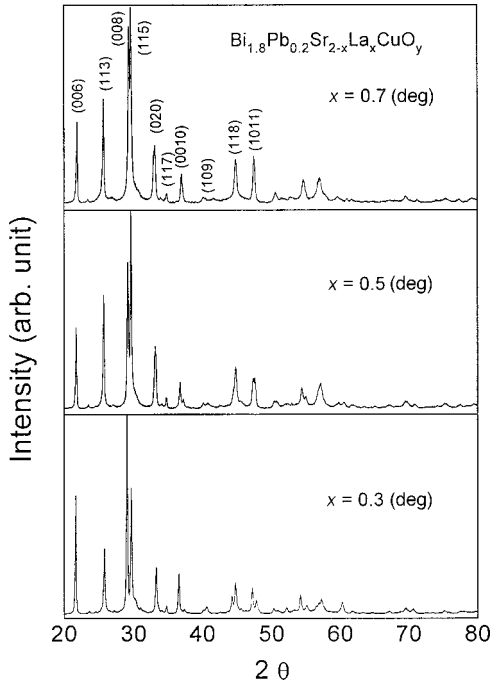

FIG. 1. XRD patterns for the $Bi_{1.8}Pb_{0.2}Sr_{2-x}La_xCuO_y$ samples with $x=0.3$, 0.5, and 0.7.

The mass densities of the Sr-vacant and La-doped Bi2201 samples were obtained by precision balance based on the buoyancy force formula: $m_{1g}-m_{2g}=v\rho g$: here, m_1 is the mass as the sample is in air, m_2 is the mass as the same sample is soaked in water, ρ is the water's mass density (1×10^3 kg/m^3), g is the gravitational constant (9.8 N/kg), and v is the sample's volume. Thus the mass density of the sample can be calculated: m_I/v.

III. EXPERIMENTAL RESULTS

The powder XRD patterns analysis indicate that both $Bi_{1.8}Pb_{0.2}Sr_{2-x}La_xCuO_y$ ($0.1\leqslant x\leqslant0.8$) and $Bi_{1.8}Pb_{0.2}Sr_{2-x}CuO_y$ ($0\leqslant x\leqslant0.6$) samples remain Bi2201 phase within the whole doping range. The XRD patterns for $Bi_{1.8}Pb_{0.2}Sr_{2-x}CuO_y$ samples have been reported elsewhere.[11] Figure 1 presents the XRD patterns for the $Bi_{1.8}Pb_{0.2}Sr_{2-x}La_xCuO_y$ samples with $x=0.3$, 0.5, and 0.7. Table I presents the data of the samples' mass density.

From the above analysis of the powder XRD patterns, it can be seen that the structure of the La-doped and Sr-vacant systems remains Bi2201 phase. The main difference between the two set samples is the microstructure, in which the valence state is zero as the Sr is replaced by a vacancy in the Bi2201 phase and the valence state changes from $+2$ to $+3$ as the La^{3+} substitutes Sr^{2+} in the Bi2201 phase.

Figure 2 shows the temperature dependence of the resistivity for the $Bi_{1.8}Pb_{0.2}Sr_{2-x}La_xCuO_y$ samples. It can be seen that the magnitude of the $\rho(T)$ values increases with x in $Bi_{1.8}Pb_{0.2}Sr_{2-x}La_xCuO_y$ samples. For the samples with $0\leqslant x\leqslant0.6$ (lines $a-f$), their $\rho(T)$ curves display approximately linear behavior at the normal state. For $x=0.75$ and 0.8 samples (lines h and i), the $\rho(T)$ exhibits weaker temperature-dependent behaviors at the higher temperature, and a semiconductorlike behavior is observed at lower temperature for the sample with $x=0.8$. All the samples display superconductivity in the doping range of $0.1\leqslant x\leqslant0.8$ (lines $a-i$). Figure 3 presents the diagram of the midpoint T_c vs the La content x obtained from Fig. 2. It is observed that the carrier concentration in the $Bi_{1.8}Pb_{0.2}Sr_{2-x}La_xCuO_y$ system covers a large range from the overdoped region to the underdoped region by varying the La content x. The variation of T_c exhibits a typical inverted parabolic behavior as the La content, i.e., the carrier concentration, changes. Table II presents the breadth of the superconductive transition: $\Delta T\,(\mathrm{K})=T^{\mathrm{onset}}_{(90\%\,\rho)}-T^{\mathrm{onset}}_{(10\%\,\rho)}$, where ρ^{onset} is the onset resistivity of the superconductive transition.

TABLE I. Mass density for the Sr-vacant and La-doped systems.

Sr or La content in two systems x	Sr-vacant samples Mass density [$10^3\times$kg/m^3]	La-doped samples Mass density [$10^3\times$kg/m^3]
0.00	5.866	5.866
0.10	5.907	5.891
0.20	5.916	6.027
0.30	5.935	6.103
0.40	6.187	
0.45	6.741	6.177
0.50	7.0735	
0.55		6.376
0.60	7.105	6.536
0.65		6.628
0.70		
0.75		6.899
0.80		7.491

Figure 4 shows the temperature dependence of the resistivity for $Bi_{1.8}Pb_{0.2}Sr_{2-x}CuO_y$ samples with $x=0.0-0.6$. It can be observed that the resistivity shows a systematic change with decreasing Sr content. The superconductive transition temperature T_c is 15.2 K for the sample with $x=0.0$ (line a). For the other samples with $x\geqslant0.1$ (lines

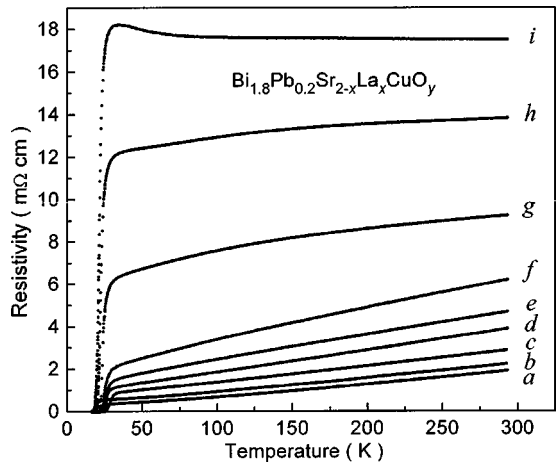

FIG. 2. The temperature dependence of resistivity for the samples with $0.1\leqslant x\leqslant0.8$ (a, $x=0.1$; b, $x=0.2$; c, $x=0.3$; d, $x=0.45$; e, $x=0.55$; f, $x=0.60$; g, $x=0.65$; h, $x=0.75$; and i, $x=0.8$).

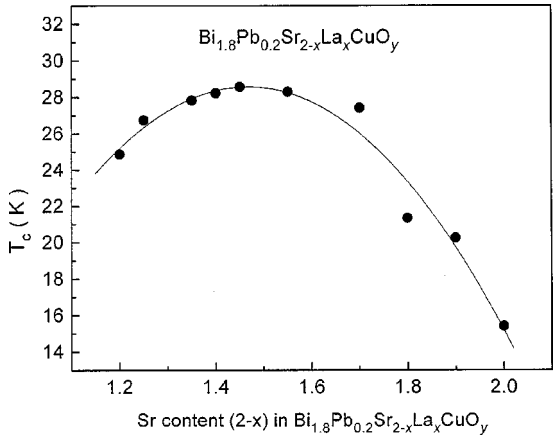

FIG. 3. Variation of the midpoint T_c as a function of x in the $Bi_{1.8}Pb_{0.2}Sr_{2-x}La_xCuO_y$ samples. The line is the guide for the eye.

$b-h$), no superconductivity appears even at the low temperature of 4.2 K. The temperature dependences of the resistivity for the samples with $x=0.0$ and 0.1 in the temperature range of 4.2–40 K are shown in the inset of Fig. 4. Additionally, it can be observed in Fig. 4 that the further decrease of the Sr content influences the normal-state transport properties of the $Bi_{1.8}Pb_{0.2}Sr_{2-x}CuO_y$ samples tremendously. The resistivity exhibits a typical linear temperature behavior for the samples with $0.1\leqslant x\leqslant 0.4$ (lines $b-e$). The resistivity shows semiconductorlike features at low temperature for samples with $x=0.45$, 0.5, and 0.6 (lines *f*, *g*, and *h*).

The measurements of the above resistivity show that the Sr vacancy influences the superconductivity more extraordinarily than the La doping in the Bi2201 phase. Raman scattering is an effective and direct method in obtaining information about the Sr site: hence, the Raman spectra are investigated for the two sets of samples.

Figures 5 and 6 present the Raman spectra for $Bi_{1.8}Pb_{0.2}Sr_{2-x}La_xCuO_y$ samples with $0.1\leqslant x\leqslant 0.75$ and for $Bi_{1.8}Pb_{0.2}Sr_{2-x}CuO_y$ samples with $0.1\leqslant x\leqslant 0.6$, respectively. Three Raman peaks around 303, 460, and 625 cm^{-1} can be clearly observed within the frequency range of 150–800 cm^{-1} in both figures. As is observed in Figs. 5 and 6, the peaks around 303 and 625 cm^{-1} are broadened and their intensities are reduced as x increases in both systems. The marked difference in both figures is that the peaks at 460 cm^{-1} do not display obvious changes in the Sr-vacant system and shoulder peaks appear at 645 cm^{-1} in the La-doped system. These shoulder peaks are generally considered as due to the insertion of the extra oxygen in Bi_2O_2 layers.

Figures 7 and 8 show the [001]-zone-axis ED patterns of the $Bi_{1.8}Pb_{0.2}Sr_{2-x}La_xCuO_y$ samples with $x=0.1-0.75$ and $Bi_{1.8}Pb_{0.2}Sr_{2-x}CuO_y$ samples with $x=0.0$, 0.3, and 0.5, respectively. The satellite sequences can be clearly observed in these ED patterns, which means that the incommensurate modulation structure exists in both systems. The average

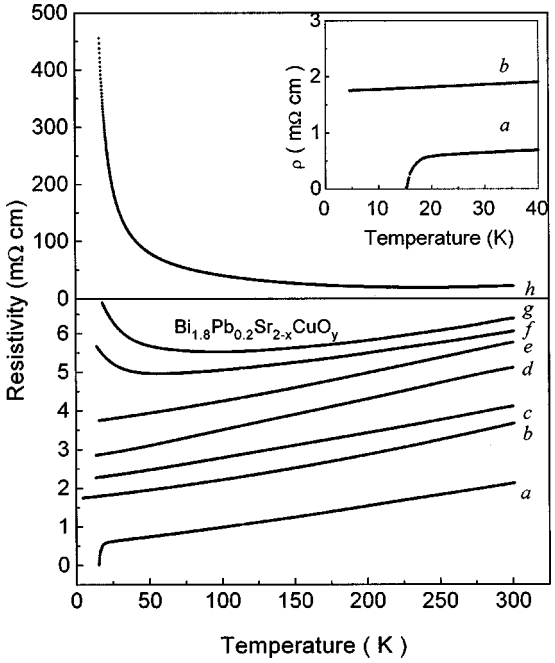

FIG. 4. The temperature dependence of resistivity for the $Bi_{1.8}Pb_{0.2}Sr_{2-x}CuO_y$ samples with $0.0\leqslant x\leqslant 0.6$ (*a*, $x=0$; *b*, $x=0.1$; *c*, $x=0.2$; *d*, $x=0.3$; *e*, $x=0.4$; *f*, $x=0.45$; *g*, $x=0.5$; and *h*, $x=0.6$). The inset shows the temperature dependence of resistivity for the samples with $x=0.0$ and 0.1 within the temperature range of 4.2–40 K.

wavelengths of the incommensurate modulation are 7.89*b*, 6.96*b*, 5.33*b*, 4.68*b*, 4.55*b*, and 4.20*b* for the $Bi_{1.8}Pb_{0.2}Sr_{2-x}La_xCuO_y$ samples with $x=0.1-0.75$, respectively, and 7.83*b*, 7.62*b*, and 7.52*b* for the $Bi_{1.8}Pb_{0.2}Sr_{2-x}CuO_y$ samples with $x=0.0$, 0.3, and 0.5, respectively.

IV. RESULTS AND DISCUSSION

The incommensurate modulation in Bi-based systems can influence the superconductivity, and it is commonly believed that the greater the change of the wavelength is, the more the superconductivity will be influenced.[12,13] However, our experimental data show controversial results. Because the changes of the wavelength in the La-doped system are much larger than that in the Sr-vacant system, this seems to suggest that the superconductivity should be influenced more markedly in the La-doped system than in the Sr-vacant system.

Using the assignment of the Raman modes in the Bi2201 phase made by Kakihana and co-workers,[14,15] the peak around 626 cm^{-1} corresponds to the A_{1g} vibration mode of the O_{Sr} atom along the *c* axis, the peak around 460 cm^{-1} is attributed to the A_{1g} vibration mode of the O_{Bi} along the *c* axis, and the peak at 303 cm^{-1} is considered as the mode of the ''extra'' phonon which is connected to the strongly dis-

TABLE II. Breadth of the superconductive transition for the La-doped system $[\Delta T\,(\mathrm{K})=T^{\mathrm{onset}}_{(90\%\ \rho)}-T^{\mathrm{onset}}_{(10\%\ \rho)}\,(\mathrm{K})]$.

x	0.0	0.1	0.2	0.3	0.45	0.55	0.6	0.65	0.75	0.8
ΔT (K)	2.38	2.697	2.807	3.108	2.957	3.086	3.128	3.198	3.173	3.119

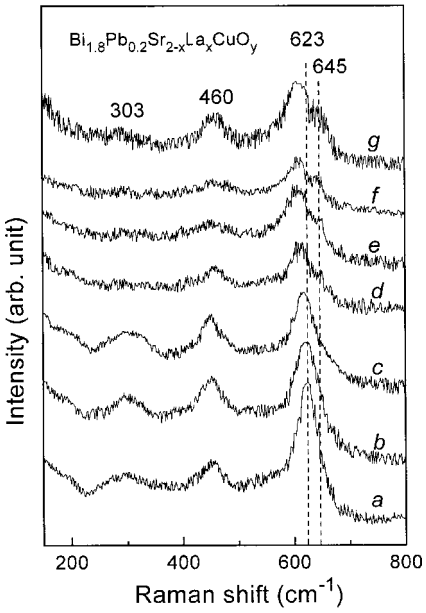

FIG. 5. Raman scattering spectra of $Bi_{1.8}Pb_{0.2}Sr_{2-x}La_xCuO_y$ samples (a, $x=0.1$; b, $x=0.2$; c, $x=0.3$; d, $x=0.45$; e, $x=0.55$; f, $x=0.65$; and g, $x=0.75$).

torted and nonideal structure of the Bi2201 (O_{Sr} refers to oxygen atom in the SrO_2 layer, O_{Bi} refers to oxygen atom in the BiO_2 layer, and O_{Cu} refers to the oxygen atom in the CuO_2 plane).

As is well known, an incommensurate superstructure generally exists in Bi cuprates, which will bring about distortion of the microstructure.[6,10,16] The average valence state in the Sr site is changed by La doping and Sr vacancy in both systems, the integrated Sr-O bond in the SrO_2 layers would be affected, and a distortion of the Sr-O bond would inevitably take place. Therefore, the appearance of peaks around 303 cm^{-1} in Raman spectra directly reflects the distortion of the microstructure induced by the La doping and Sr vacancy in the SrO_2 layers.

The substitution of aliovalent cations with different radius

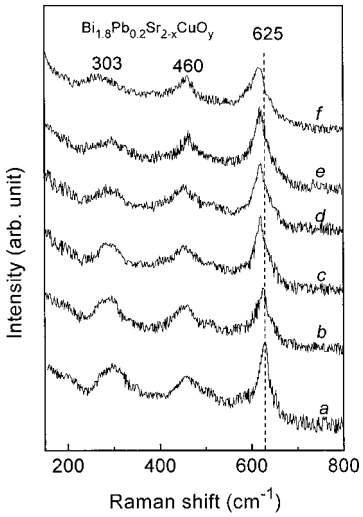

FIG. 6. Raman scattering spectra of $Bi_{1.8}Pb_{0.2}Sr_{2-x}CuO_y$ samples (a, $x=0.1$; b, $x=0.2$; c, $x=0.3$; d, $x=0.4$; e, $x=0.5$; and f, $x=0.6$).

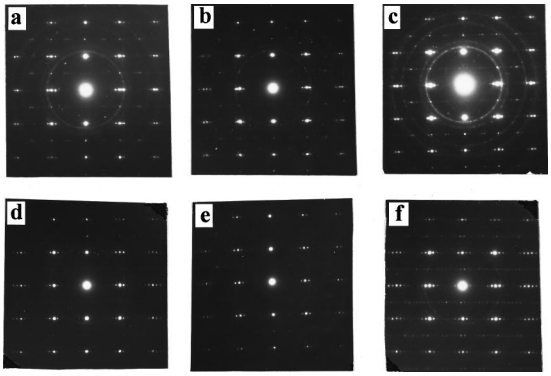

FIG. 7. [001]-zone-axis ED patterns of $Bi_{1.8}Pb_{0.2}Sr_{2-x}La_xCuO_y$ samples (a, $x=0.1$; b, $x=0.2$; c, $x=0.3$; d, $x=0.45$; e, $x=0.65$; and f, $x=0.75$).

and different valence in the Sr site will inevitably bring about a charge redistribution and changes of some bond lengths in the Bi2201 phase. Then the corresponding frequency of some Raman modes in the Bi2201 phase should be closely related to such changes.

The SrO_2 layer is directly coupled to the upper Bi_2O_2 layers and the lower CuO_2 plane in the Bi2201 phase. Hence the changes of the average valence state in the Sr site will not only influence the SrO_2 layer itself, but also influence the upper Bi_2O_2 layers and lower CuO_2 plane at the same time. Let us first examine how the SrO_2 layer itself is influenced by the La doping and the Sr vacancy in the Sr site. About the changes of the modes around 625 cm^{-1} in both systems, from a structural point of view this is unexpected: the average ionic radius in the Sr site should be reduced either by La doping or Sr vacancy, because r_{Sr}^{2+} is 1.26 Å and r_{La}^{3+} is 1.16 Å, $r_{La}^{3+}/r_{Sr}^{2-}<1$, and $r_{Sr2-x}^{2-}/r_{Sr2}^{2+}<1$; in other words, La doping and Sr vacancy should lead to a reduction of the average radius in the Sr site in the Bi2201 phase. The reduction in the average ionic radius in the Sr site should push the O_{Sr} phonon higher in frequency. However, we observe that the modes of the O_{Sr} phonon shift towards lower frequency as the La content and Sr vacancy are introduced in Sr sites in both systems. So the behaviors of the peaks around 625 cm^{-1} should be attributed to changes of the average valence state in the Sr site. It is known that the La^{3+} substitution for Sr^{2+} in the Bi2201 phase should increase the average valence state in the Sr site, and the Sr vacancy in the Sr site should decrease the average valence state of the Sr site. Band-structure calculations[8,17] indicate that the metallic state extends over the whole O_{Cu}-Cu-O_{Sr}-Bi-O_{Bi} complex. Doping electrons into this complex induced by La doping would increase the average electron density on Cu and Bi, and doping holes into this complex induced by Sr vacancy would in-

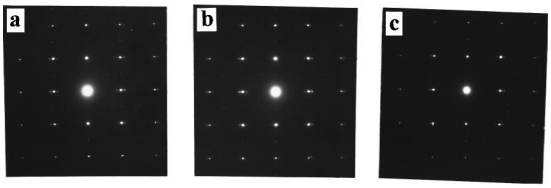

FIG. 8. [001]-zone-axis ED patterns of $Bi_{1.8}Pb_{0.2}Sr_{2-x}CuO_y$ samples (a, $x=0.0$; b, $x=0.3$; and c, $x=0.5$).

crease the average hole density on O_{Sr}, O_{Cu}, and O_{Bi}. Such circumstances will decrease the electrostatic attraction in the O_{Cu}-Cu-O_{Sr}-Bi-O_{Bi} complex. This should result in a softening of the O_{Sr} mode. Hence the peaks around 625 cm^{-1} shift toward lower frequency as the La and Sr vacancies are introduced in the Sr sites in the Bi2201 phase.

On the other hand, there is a coupling between the Bi_2O_2 layer and perovskitelike blocks: therefore, changes of the average valence in the Sr site induced by the La doping and Sr vacancy should also influence the upper Bi_2O_2 layer. As a result, the peaks of the O_{Bi} modes in the Bi_2O_2 layers will inevitably be affected. Hence let us investigate the behavior of the upper Bi_2O_2 layer as the La and Sr vacancies are introduced in the Sr site in the Bi2201 phase. For the $Bi_{1.8}Pb_{0.2}Sr_{2-x}CuO_y$ system, the O_{Bi} is in the Bi_2O_2 layer and the O_{Sr} is in the perovskitelike blocks. The influence of the changes in the average charge density around the O_{Sr} site should be weaker on the O_{Bi} atom than on the O_{Sr} atom as the Sr content decreases. Therefore, there are no obvious changes in the peaks of the O_{Bi} around 460 cm^{-1} as shown in Fig. 6. But in the $Bi_{1.8}Pb_{0.2}Sr_{2-x}La_xCuO_y$ system, the Bi_2O_2 layer should be influenced by the changes of the average valence state in the Sr site induced by the La doping. The average valence state in the Sr site will change from $+2$ to $+3$ as Sr^{2+} is replaced by La^{3-}. As a result, superfluous $+1$ valence appears in the Sr(La^{3+}) site. Extra oxygen has to enter the crystal in order to balance this superfluous $+1$ valence in the Sr(La^{3+}) site. However, extra oxygen cannot enter the SrO_2 layers because the Sr site and the O_{Sr} site in the SrO_2 layer have been occupied; instead, extra oxygen has to be inserted into the Bi_2O_2 layers. Therefore, extra oxygen peaks can be observed clearly at the 645 cm^{-2} in Fig. 5. The insertion of the extra oxygen in the Bi_2O_2 layers reduces the electronic Raman scattering background of the O_{Bi} modes, forms the structural modulation, and increases the length of the Br-O bond. So the intensity of the peaks around 460 cm^{-1} exhibits a decreasing trend as the La content increases in the $Bi_{1.8}Pb_{0.2}Sr_{2-x}La_xCuO_y$ system. Nevertheless, in the Sr-vacant system the oxygen content in the Bi_2O_2 layer cannot be changed as the Sr vacancy increases. Hence the peaks at the 460 cm^{-1} in Fig. 6 display no obvious changes for the $Bi_{1.8}Pb_{0.2}Sr_{2-x}CuO_y$ system.

From analysis of Raman scattering and ED, it can be easily understood how the changes of the average valence state in the Sr site influence the superconductivity in the La-doped and Sr-vacant systems. As is discussed above, La substitution for Sr only brings about the insertion of the extra oxygen and the formation of the incommensurate modulation in the Bi_2O_2 layers, but the microstructure characteristic of the CuO_2 planes cannot be directly influenced. The direct effect induced by the La doping is that the carrier concentration is varied from the overdoped region to the underdoped region as shown in Fig. 3.

As the La content, i.e., the carrier concentration, changes, the variation of the T_C exhibits a typical inverted parabolic behavior which has been observed in most of the HTSCs. Comparing our data of T_C for the Pb-doped $Bi_{1.8}Pb_{0.2}Sr_{2-x}La_xCuO_y$ system with other reported data of the T_C for the Pb-free $Bi_2Sr_{2-x}La_xCuO_y$ system from Subramaniam *et al.*,[18] Groen *et al.*,[19] Maeda *et al.*,[20] and Sastry *et al.*,[21] it can be clearly noticed that our T_C is the highest in these five data. It is suggested that this may arise from the effects of Pb doping in the Bi2201 phase. It is known that La doping in the Bi2201 phase can bring about two effects: the changes of the carrier concentration and the intensification of the structural distortion. The former can improve the superconductivity, and the latter can destroy the superconductivity. However, in contrast with the two effects, the improvement of the superconductivity induced by the former offsets the destruction of the superconductivity induced by the latter. Therefore, La doping is effective in increasing the T_C. Additionally, if the structural distortion is relaxed, further increase of the T_C is possible. It is well known that Pb doping in Bi-based cuprates can depress the incommensurate modulation and can also systematically raise the T_C of the Bi-based superconductors.[13,22] Hence the further increase of the T_C may arise from the depression of the incommensurate modulation through the Pb doping in the $Bi_{1.8}Pb_{0.2}Sr_{2-x}La_xCuO_y$ system. The fact that La and Pb doping can raise the T_C suggests that the superconductivity depends not only on the carrier concentration in the system, but also on the microstructural characteristics of the crystal structure. Similar effects of the increase in T_C induced by Pb doping have also been observed in the Bi2212 system,[20] Bi2201 system,[22] and T12201 system.[23]

No superconductivity appears even at 4.2 K for the lowest x in the $Bi_{1.8}Pb_{0.2}Sr_{2-x}CuO_y$ system. This indicates that the superconductivity and the normal-state transport properties are very sensitive to the Sr vacancy in the $Bi_{1.8}Pb_{0.2}Sr_{2-x}CuO_y$ samples. Why does the Sr vacancy suppress the superconductivity so tremendously in this system? We suggest that such a suppression of the superconductivity originates from a shift of the apical oxygen of the CuO_6 octahedron induced by the Sr vacancy in the $Bi_{1.8}Pb_{0.2}Sr_{2-x}CuO_y$ samples. As is known, the CuO_2 plane is mainly responsible for the superconductivity and the normal-state transport properties for the HTSCs. In the Bi2201 phase, the O_{Sr} in the SrO_2 layer is the apical oxygen of the CuO_6 octahedron. As the Sr vacancy is introduced in the Sr site, the O_{Sr} will shift and, as a result, the shifts of the apical oxygen of the CuO_6 octahedron will directly influence the CuO_2 planes. Thus the conducting behavior of the charge carriers in the CuO_2 plane will, of course, be changed tremendously. Therefore, the superconductivity and the normal-state transport properties will be influenced extraordinarily due to the Sr vacancy in the Sr site. Recently, Hiroyuki[24] has investigated the new members of Sr-free Bi-based cuprates with the 2201 structure and find that the superconductivity will immediately disappear as the Sr site is replaced by other cation elements Na and K. His studies indicated that the samples show a temperature dependence of $\ln \rho \alpha T^{-1/4}$ without any trace of the superconductivity even down to 5 K as the Sr is completely replaced by cation elements Na and K. The reason for this may be a distortion of the CuO_6 octahedron induced by the Na and K doping in the Sr site. Therefore, the disappearance of the superconductivity in the $Bi_{1.8}Pb_{0.2}Sr_{2-x}CuO_y$ samples should be attributed to the strong distortion of the CuO_6 octahedron. This distortion would make the apical oxygen atom diverge from its equilibrium site in the crystal structure. However, in the $Bi_{1.8}Pb_{0.2}Sr_{2-x}La_xCuO_y$ samples, La substitution in the Sr

site belongs to pure electronic doping and the CuO_6 octahedron is not distorted so strongly by the La doping. So the superconductivity and the normal-state transport properties are mainly dominated by the changes of the carrier concentration in the La-doped Bi2201 system.

V. CONCLUSION

In summary, Raman scattering, ED, and the resistivity for Bi2201 phases have been investigated. The two effects induced by the La doping and Sr vacancy in the Sr site are quite different: both the La doping and the Sr vacancy result in the changes of the average valence state in the Sr site; however, La doping is pure electronic filling in the system, and the superconductivity and the normal-state transport properties are mainly dominated by the changes of the carrier concentration in the $Bi_{1.8}Pb_{0.2}Sr_{2-x}La_xCuO_y$ system. Nevertheless, the superconductivity is suppressed strongly in the $Bi_{1.8}Pb_{0.2}Sr_{2-x}CuO_y$ system, which suggests that the Sr vacancy in the Sr site leads to a shift of the apical oxygen of the CuO_6 octahedron. Our experimental data and analysis further indicate that the microstructural characteristic is very important for the superconductivity and the normal-state transport properties of the HTSCs.

ACKNOWLEDGMENTS

This work was supported by the National Center for Research and Development on Superconductivity and the National Natural Science Foundation of China, Grant No. 59625205.

[1] B. Batlogg, Phys. Today **44** (6), 44 (1991).
[2] J. B. Goodenough, Supercond. Sci. Technol. **3**, 26 (1990).
[3] E. N. Van Eenige, R. Griessen, R. J. Wijngaarden, J. Karpinski, E. Kaldis, S. Rusiecki, and E. Jilek, Physica C **168**, 482 (1990).
[4] A. J. Millis and K. M. Rabe, Phys. Rev. B **38**, 8908 (1988).
[5] H. J. Kim and R. Moret, Physica C **156**, 363 (1988).
[6] M. Ido, N. Yamada, M. Oda, Y. Segawa, N. Momono, A. Onodera, Y. Okajima, and K. Yamaya, Physica C **185–189** (1991).
[7] Mao Zhiqiang, Tian Mingliang, Ji Mingrong, Zhu Jingsheng, Zuo Jian, Wang Ruiping, Wang Wu, and Zhang Yuheng, Phys. Rev. B **49**, 9857 (1994).
[8] W. E. Pickett, Rev. Mod. Phys. **61**, 433 (1989).
[9] J. D. Jorgemsen, Phys. Today **44** (6), 34 (1991).
[10] M. Cardona, R. Liu, R. Liu, H. G. Von Schnering, M. Hartweg, Y. F. Yan, and Z. X. Zhao, Solid State Commun. **66**, 1225 (1988).
[11] Yan Hongjie, Mao Zhiqiang, Xu Gaojie, and Zhang Yuheng, Phys. Rev. B **59**, 8459 (1999).
[12] Mao Zhiqiang, Fan Chenggao, Shi Lei, Yao Zhen, Yang Li, Wang Yu, and Zhang Yuheng, Phys. Rev. B **47**, 14 467 (1993).
[13] Mao Zhiqiang, Xu Gaojie, Zhang Shuyuan, Tan Shun, Lu Bin, Tian Mingliang, Fan Chenggao, Xu Cunyi, and Zhang Yuheng, Phys. Rev. B **55**, 9130 (1997).
[14] Masato Kakihana, Minoru Osada, Mikael Kall, Lars Börjesson, Hiromasa Mazaki, Hiroshi Yasuoka, Masatomo Yashima, and Masahiro Yoshimura, Phys. Rev. B **53**, 11 796 (1996).
[15] Minoru Osada, Masato Kakihana, Mikael Kall, Lars Börjesson, Atsuyoshi Inoue, and Masatomo Yashima, Phys. Rev. B **56**, 2847 (1997).
[16] L. A. Farrow, R. Ramesh, and J. M. Tarascon, Phys. Rev. B **43**, 418 (1991).
[17] P. A. Sterne and C. S. Wang, Physica C **21**, L949 (1988).
[18] C. K. Subramaniam, C. V. N. Rao, A. B. Kaiser, H. J. Trodahl, A. Mawdsley, N. E. Flower, and J. L. Tallon, Supercond. Sci. Technol. **7**, 30 (1994).
[19] W. A. Groen, D. M. de Leeuw, and G. M. Stollman, Solid State Commun. **72**, 697 (1989).
[20] A. Maeda, M. Hase, I. Tsukada, K. Noda, S. Takebayashi, and K. Uchinokura, Phys. Rev. B **41**, 6418 (1990).
[21] P. V. P. S. S. Sastry, J. V. Yakhmi, R. M. Iyer, C. K. Subramaniam, and R. Srinivasan, Physica C **178**, 110 (1991).
[22] Xu Gaojie, Mao Zhiqiang, Xu Xiaojun, Tian Mingliang, Shi Lei, and Zhang Yuheng, J. Phys.: Condens. Matter **9**, 5137 (1997).
[23] T. Kaneko, T. Wada, A. Ichinose, H. Yamauchi, and S. Tanaka, Physica C **177**, 153 (1991).
[24] Hiroyuki Sasakura, Physica C **292**, 125 (1997).